# Revealing Protein Structures in Solid-phase Peptide Synthesis by ^{13}C Sold-state NMR: Evidence of Excessive Misfolding for Alzheimer's β

**Songlin Wang**[1] and **Yoshitaka Ishii**[1],[2],[*]

[1]Department of Chemistry, University of Illinois at Chicago, 845 West Taylor Street Chicago, Illinois 60607

[2]Center for Structural Biology, University of Illinois at Chicago, 1100 South Ashland Street, Chicago IL 60607

## Abstract

Solid-phase peptide synthesis (SPPS) is a widely used technique in biology and chemistry. However, the synthesis yield in SPPS often drops drastically for longer amino acid sequences, presumably due to the occurrence of incomplete coupling reactions. The underlying causes for this problem are hypothesized to be a sequence-dependent propensity to form secondary structures through protein aggregation. However, few methods are available to study the site-specific structure of proteins or long peptides that are anchored to the solid support used in SPPS. This study presents a novel solid-state NMR (SSNMR) approach to examine protein structure in the course of SPPS. As a useful benchmark, we describe the site-specific structural characterization of the 40-residue Alzheimer's β-amyloid (Aβ) peptide during SPPS by SSNMR. Our 2D ^{13}C/^{13}C correlation SSNMR data on Aβ(1-40) bound to a resin support demonstrated that Aβ underwent excessive misfolding into a highly ordered β-strand structure across the entire amino-acid sequence during SPPS. This approach is likely to be applicable to a wide range of peptides/proteins bound to the solid support that are synthesized through SPPS.

Solid-phase peptide synthesis (SPPS) has been proven to be a highly effective technique for the production of proteins/peptides of an arbitrary amino-acid sequence at high purity[1]. More recently, SPPS has been an indispensable tool for the construction of peptide/protein libraries for high-throughput screening in systems biology and drug development.[2] On the other hand, it is known that coupling efficiency in SPPS is radically suppressed for long peptide sequences that exceed 30–50 residues[3]. Thus, chemical synthesis of a protein having a longer amino-acid sequence often requires chemical ligation of shorter peptides[4], which limits automation and high-throughput applications that are crucial in modern biology. The difficulties in the synthesis of longer peptides have been attributed to secondary structure formation through inter-chain aggregation and/or poor solvation of the growing peptide chains[3,5]; however the detailed molecular mechanisms responsible for these observations are currently unknown. For example, a peptide in SPPS is elongated from the C-terminus to the N-terminus by repeated coupling of Fmoc- or Boc-protected amino acids; thus, a major hindrance from the hypothesized misfolding in SPPS should arise from the structural transition or the lack of solvation at the N-terminal regions. On the other hand, the N-terminal regions of proteins are often unstructured[6] and less likely to participate in the

yishii@uic.edu.

expected structure formation in SPPS. Therefore, site-specific structures of peptides/proteins in SPPS will provide valuable molecular-level insight into the controversies and challenges of synthesizing larger peptides or proteins.

Currently, very little is known about the structure of a protein or a long peptide (> 20 residues) during SPPS, despite recent advances in structural biology. X-ray crystallography, a powerful method for protein structural determination, is not an option because of the non-crystalline nature of heterogeneous solid-support in SPPS. Characterization of peptides/ proteins during SPPS by solution NMR or other spectroscopic methods have been generally limited because of the solid support, such as resin, which absorbs or scatters light and limits the resolution of solution NMR. A wide-line [2]D solid-state NMR (SSNMR) study for resin-bound polyglycine $[(gly-d_2)_n]$ (n = 3–9) indicated a loss of mobility for the system when a critical length was exceeded $(n > 5)$[7], yet without any structural details or site specificity. High-resolution solution NMR[8] has been used to characterize resin-bound polyalanine[9] or saccharides.[10] However, the application of this method has been limited to only very short peptides (up to 10–15 residues) because of the restricted resolution for longer sequences. Thus, it has been an intractable problem of defining a detailed site-specific structure on a long peptide or protein in SPPS for nearly 50 years since the introduction of SPPS by Merrifield[1].

In this study, we propose high-resolution ^{13}C SSNMR analysis of resin-bound proteins during SPPS in order to achieve the site-specific structural analysis for such systems. As an interesting benchmark, we selected the 40-residue β-amyloid (Aβ) peptide because it is one of only a few biologically significant systems for which structures of both monomeric and misfolded forms have been reported. It is well-known that unstructured monomeric Aβ (1-40) self-assembles into β-sheet rich amyloid fibrils, which are associated with Alzheimer's disease (AD).[11] Because of great interest in Aβ for biomedical and biophysical studies,[11,12] including SSNMR studies[13,14], the Aβ peptide has been a major target of SPPS.[15] Indeed, various SPPS methods were proposed to overcome difficulties in SPPS.[16] However, there has been little experimental evidence about structural features of Aβ in SPPS, which may provide critical insights into the mechanism that prevents SPPS for Aβ and other long peptides. Here, with recent progress in biomolecular SSNMR[17], we revisit this long-standing problem. We report that ^{13}C SSNMR analysis using magic angle spinning (MAS) serves as a probe that is very sensitive to site-specific structural properties of proteins in SPPS.

Figure 1(a, b) shows (a) 1D ^{13}C CPMAS and (b) 2D ^{13}C/^{13}C correlation SSNMR spectra of resin-bound Aβ (1-40) peptide labeled at several sites between residues 19–34 with uniformly [13]C- and ^{15}N-labeled amino acids. (see the caption). The sample was prepared by standard Fmoc-based SPPS using Wang resin as a solid support (see the Materials and Methods and Supporting Information (SI) for details), and packed in a rotor after washing with dichloromethane (DCM). As mentioned above, the C-terminus of a peptide is bound to resin in Fmoc-based SPPS, and Fmoc protected amino acids are repeatedly coupled to the N-terminus (Fig. 1d). Thus, these labeled sites reflect peptide conformations closer to the resin support. In monomeric form, Aβ (1-40) is known to largely exhibit a random-coil structure with high degree of dynamics.[20] Initially, we expected considerable dynamics and structural heterogeneity for the resin-bound peptide solvated with DCM, resulting in weaker and broader ^{13}C signals in the ^{13}C CPMAS spectra. Unexpectedly, however, the strong signal intensities were observed in the 1D ^{13}C CPMAS spectrum (Fig. 1a); this confirmed the lack of motions in the area, because large-amplitude motions would have averaged out dipolar couplings and suppressed ^{13}C signals through cross polarization. More surprisingly, the cross peaks for the 2D ^{13}C/^{13}C SSNMR spectrum (Fig. 1b) showed reasonably narrow line widths (1.9–2.8 ppm), considering that the system embedded in resin is non-crystalline, and

that the line widths include Gaussian broadening (ca. 1 ppm) and broadening due to $^{13}C$-$^{13}C$ J couplings. The line widths were comparable to those of Aβ (1-40) amyloid fibrils, which are known to have a high degree of structural order.[19,21] Because chemical shifts are sensitive to conformations of a peptide, this finding clearly suggests the formation of a highly ordered conformation, which has not been predicted in previous studies for this system bound to a heterogeneous resin matrix.

Using the well-resolved resonances and signal assignments shown in Fig. 1b, we analyzed secondary structures of resin-bound Aβ (1-40) using secondary $^{13}C$ shifts (Δ) for $^{13}C_\alpha$ (blue) and $^{13}C_\beta$ (red) shifts, which represent the deviation of the experimental shift ($\delta_{exp}$) from the corresponding shift for random-coil model peptides ($\delta_{rc}$)[22] (i.e. $\Delta = \delta_{exp} - \delta_{rc}$; see also SI in Table S1). Negative and positive Δ values for $^{13}C_\alpha$ and $^{13}C_\beta$, respectively, suggest the formation of extended β-strand structures over the hydrophobic core region in Aβ (1-40).[22] It is noteworthy that in Fig. 1b, only a single cross peak was observed for a chemically bonded $^{13}C$-$^{13}C$ pair, unlike some amyloid fibrils, which often show multiple cross peaks for a $^{13}C$-$^{13}C$ pair due to structural polymorphs. This result suggests a remarkable finding that the Aβ (1-40) peptide not only aggregates in the course of SPPS, but also misfolds into a single, well-defined β-strand conformer. For the SPPS of Aβ, we used low-loading resin (0.22 meq/g in a dry state), yet the estimated concentration of Aβ in resin swollen with a solvent is in a range of 40 mM, which is typically more than sufficient to introduce misfolding of Aβ (1-40) in an aqueous solution. On the other hand, peptides from SPPS have very limited translational diffusion unlike a peptide in a solution due to the solid-support. Thus, it was not trivial to predict misfolding and a high degree of structural order for Aβ in SPPS. The features of this SSNMR spectrum, which was collected approximately 2 h after the synthesis, were unaltered over several days (see Fig. S4 in SI). This result suggests that the peptides were misfolded, and their conformation reached the equilibrium state in the solvent reasonably quickly. We confirmed that with the exception of mild line broadening, the chemical shifts for this sample were unchanged by the removal of DCM (Fig. S4c). We also collected a 1D $^{13}$CPMAS spectrum of the same resin-bound Aβ peptide sample solvated with NMP, which was obtained without a DCM wash, although the flammable nature of NMP prevented us from testing a time-consuming 2D experiment. The 1D spectrum for this sample with NMP was found to be very similar to that shown in Fig. 1a. Thus, the solvent effects on $^{13}C$ shifts are negligible. Of note, the β-strand structures are likely stable without the solvents.

We next examined the site-specific structure of the N-terminal residues of Aβ (1-40) in SPPS. In previous studies on amyloid fibrils, it was reported that the first 10 residues of Aβ (1-40) in the N-terminus are disordered or mobile[19]. On the other hand, we found that it was difficult to efficiently couple the last 3–4 amino acids of the N-terminus of Aβ (1-40) in SPPS without multiple couplings. Therefore, we decided to examine whether misfolding of Aβ in SPPS involves three residues (Ala-2, Phe-4, Val-12) in the N-terminal region using 2D $^{13}C$/$^{13}C$ correlation SSNMR for Aβ (1-40) for which uniformly $^{13}C$- and $^{15}N$-labeled amino acids were introduced at these sites (Fig. 2a). Although the normalized signal intensities were weaker than those observed in Fig. 1b, sharp resonances were observed for the cross peaks for all of these esidues. Surprisingly, analysis of the secondary chemical shifts for $^{13}C_\alpha$ and $^{13}C_\beta$, exhibited negative and positive shifts, respectively (Fig. 2b), suggesting the formation of a β-strand in the N-terminal region up to Ala-2. Quantitative analysis using TALOS software also confirmed the β-strand formation (Table S1). This finding confirms the excessive misfolding of the N-terminal residues of Aβ (1-40) in SPPS, which has not been previously observed, even for the Aβ (1-40) fibril. This is the first example that demonstrates excessive misfolding of the β-strand in the N-terminal region for a relatively long peptide in SPPS.

These new data indicate that some dynamics are involved in the N-terminal region of Aβ when bound to resin. We first noticed that the signal-to-noise ratio in Fig. 2a was less than that in observed in Fig. 1b for the unit sample and unit number of scans. The integrated signal intensity of the aliphatic region (10–70 ppm) in the 1D spectrum normalized by sample amount and the numbers of $^{13}$C species and scans was less than what was observed in Fig. 1a (~67%). To examine the effects of solvents and dynamics, we obtained a 2D $^{13}$C/$^{13}$C spectrum for Aβ (1-40) for the same sample after removing the solvent (Fig. 2c). Interestingly, new resonances emerged for Ala-2, Phe-4, and Val-12 (dotted line for Fig. 2c) in the spectrum for the sample without the solvent. The new resonances for Phe-4, which did not have very clear separation from the peaks for Val-12 in Fig. 2c, were confirmed by a dipolar assisted rotational resonance (DARR) experiment (see Fig. S6). Remarkably, the secondary chemical shifts for these new resonances (Fig. 2d) indicate α-helical structure for Ala-2, Phe-4, and Val-12 (Table S1), based on the analysis using TALOS software.[23] The integral intensities of these peaks were comparable to those for the resonances corresponding to the β-strand structure (ca. 120% for Ala-2 with respect to the corresponding peak for the β-strand species). Slightly broader line widths observed in Fig. 2c may be attributed to the conformational heterogeneity fixed after solvent removal. The present SSNMR results suggest for the first time that unlike amyloid fibrils of Aβ, approximately half of the population of Aβ (1-40) exhibits excessive misfolding into a rigid β-strand within the N-terminal region during SPPS, while the rest of the population possesses a helical structure. Because the latter conformer is not visible in the 2D spectrum with solvent (Fig. 2a), it is likely that the highly dynamic nature of the non-β conformer suppressed the cross polarization in the presence of solvent (see also Fig. S5 in SI). Our preliminary data using $^{13}$C-$^{1}$H rotational-echo double-resonance (REDOR) experiments for $^{13}$C$_\alpha$ of Ala-2 and Ala-30 for Aβ in DCM (see SI) showed that these residues in the β-strand structures have order parameters close to 1 ($S = 0.84$–0.86; Table S2), which suggest a lack of motion. These data clearly demonstrate that the proposed novel SSNMR analysis allows us to determine the site-specific structural and dynamic information, including the presence of the two conformations in the N-terminus of Aβ during SPPS. It is quite possible that the excessive misfolding into an extended β-strand structure at the N-terminus prevents coupling of additional amino acids. In SPPS, the efficiency of coupling (*f*) for each amino acid usually needs to be extremely high ($f > 99\%$) as the yield ($\xi$) is approximately given by $\xi = (f)^N$, where N denotes the number of amino acid residues. Assuming that *f* is ca. 50% (or 0.5), the yield is suppressed down to $\xi$ of 0.8–3% even for a short sequence having 5–7 residues. The population of the misfolded species obtained by SSNMR (~50%) implies that a drastic decline in the synthesis efficiency of SPPS could be explained by the excessive misfolding across the sequence.

In conclusion, we have presented an approach for obtaining site-specific analysis of protein structures during SPPS. Despite the long history of SPPS and its effectiveness in biological applications, no site-specific structures have been reported for proteins bound to a solid-support in SPPS. We demonstrated that our SSNMR approach is highly effective in elucidating structural and dynamic features of long peptides or proteins during SPPS using Aβ (1-40) as a notable benchmark system of a long hydrophobic peptide. This is the first example reporting that a site-specific structure can be defined for aggregated proteins during SPPS. Since a relatively small quantity of isotope-labeled peptide-bound resin (5–10 mg) is required for multi-dimensional $^{13}$C SSNMR analysis, our approach opens an avenue toward the routine analysis of protein structures during SPPS. Moreover, our SSNMR data of Aβ (1-40) peptide bound to a heterogeneous resin demonstrated that the resin-bound peptide undergoes misfolding into a unique conformation having a highly ordered β-strand structure during the course of SPPS. To our surprise, the β-strand region of Aβ (1-40) bound to resin spans the entire sequence, including the N-terminal region, which is unstructured and dynamic for Aβ (1-40) even in amyloid fibrils. The observation of excessive misfolding

provides excellent insight into how the structural evolution of Aβ can interfere with efficient coupling in the N-terminus of a peptide during SPPS. These findings clearly indicate major structural problems in efficient synthesis of Aβ and possibly other proteins by SPPS. Although additional studies are needed to identify whether such excessive misfolding into highly rigid β-strand structures is commonly observed during SPPS of other peptides/ proteins, the SSNMR approach presented here is likely applicable to a broad range of proteins, and may provide a critical structural foundation for designing more efficient SPPS schemes. For analysis for long peptides with redundant amino acids, the present method using 2D $^{13}$C/$^{13}$C correlation requires a considerable number of labeled samples to examine the entire sequence, as commonly observed for SSNMR analysis of heterogeneous peptides. For such systems, sequential assignments may offer more efficient structural analysis in future studies.

## Materials and Methods

All starting materials, with the exception of isotope-labeled Fmoc-protected amino acids, were obtained from commercial suppliers and used without further purification. All of the unlabeled Fmoc-protected amino acids, HCTU, and low-density Fmoc-Val-Wang resin (0.22 meq/g) were obtained from Peptides International (Louisville, KY). Uniformly $^{13}$C- and $^{15}$N labeled amino acids were purchased from Isotec/Sigma-Aldrich (Miamisburg, OH). The Fmoc protection of the labeled amino acids was performed at the UIC Research Resource Center.[24] Piperidine was purchased from Sigma-Aldrich (St. Louise, MO). Other reagents and solvents for peptide synthesis were purchased from Applied Biosystems (ABI, Foster City, CA). $^{13}$C- and $^{15}$N-labeled Aβ(1-40) was synthesized with standard Fmoc-based synthesis as previously described[14] with an ABI 433 peptide synthesizer using the Fmoc-Val-Wang resin. After synthesis, the Fmoc-group was deprotected and the resin was washed with DCM. The purity of the peptides was tested by mass spectrometry (Fig. S1). Other details are described in the SI.

All of the SSNMR experiments were conducted at a static field of 9.4 T using a Varian InfinityPlus 400 NMR spectrometer and a home-built 2.5 mm MAS triple-resonance probe. The $^{13}$C chemical shifts were referenced to TMS using adamantine CH signal (38.56 ppm) as the secondary external reference. The MAS spinning speed was set to $20,000 \pm 3$ Hz for all of the experiments. Other details are described in the SI.

## Supplementary Material

Refer to Web version on PubMed Central for supplementary material.

## Acknowledgments

## References

1. Merrifield RB. J Am Chem Soc. 1963; 85:2149–2154.Merrifield B. Science. 1986; 232:341–347. [PubMed: 3961484]

2. Beyer M, et al. Science. 2007; 318:1888–1888. [PubMed: 18096799] Chen XY, Gambhir SS. Nat Chem Biol. 2006; 2:351–352. [PubMed: 16783336] Peng L, Liu RW, Marik J, Wang XB, Takada Y, Lam KS. Nat Chem Biol. 2006; 2:381–389. [PubMed: 16767086] Breitling F, Nesterov A, Stadler V, Felgenhauer T, Bischoff FR. Mol Biosyst. 2009; 5:224–234. [PubMed: 19225611]

3. Kent SBH. Annu Rev Biochem. 1988; 57:957–989. [PubMed: 3052294] Coin I, Beyermann M, Bienert M. Nat Protocols. 2007; 2:3247–3256.

4. Dawson PE, Muir TW, Clarklewis I, Kent SBH. Science. 1994; 266:776–779. [PubMed: 7973629]

5. Larsen BD, Christensen DH, Holm A, Zillmer R, Nielsen OF. J Am Chem Soc. 1993; 115:6247–6253.

6. Lobanov MY, Furletova EI, Bogatyreva NS, Roytberg MA, Galzitskaya OV. Plos Comput Biol. 2010; 6

7. Ludwick AG, Jelinski LW, Live D, Kintanar A, Dumais JJ. J Am Chem Soc. 1986; 108:6493–6496.

8. Keifer PA, Baltusis L, Rice DM, Tymiak AA, Shoolery JN. J Magn Reson A. 1996; 119:65–75.Sarkar SK, Garigipati RS, Adams JL, Keifer PA. J Am Chem Soc. 1996; 118:2305–2306.Fitch WL, Detre G, Holmes CP, Shoolery JN, Keifer PA. J Org Chem. 1994; 59:7955–7956.

9. Warrass R, Wieruszeski JM, Boutillon C, Lippens G. J Am Chem Soc. 2000; 122:1789–1795.

10. Loening NM, Kanemitsu T, Seeberger PH, Griffin RG. Magn Reson Chem. 2004; 42:453–458. [PubMed: 15095381]

11. Selkoe D. J Nat Cell Biol. 2004; 6:1054–1061.

12. Klein WL, Stine WB, Teplow DB. Neurobiol Aging. 2004; 25:569–580. [PubMed: 15172732] Noguchi A, et al. J Biol Chem. 2009; 284:32895–32905. [PubMed: 19759000]

13. Petkova AT, Leapman RD, Guo ZH, Yau WM, Mattson MP, Tycko R. Science. 2005; 307:262–265. [PubMed: 15653506] Parthasarathy S, Long F, Miller Y, Xiao Y, Thurber K, McElheny DBM, Nussinov R, Ishii Y. J Am Chem Soc. 2011; 133:3390–3400. [PubMed: 21341665] Ahmed M, Davis J, Aucoin D, Sato T, Ahuja S, Aimoto S, Elliott JI, Van Nostrand WE, Smith SO. Nat Struct Mol Biol. 2010; 17:561–567. [PubMed: 20383142] de Planque MRR, Raussens V, Contera SA, Rijkers DTS, Liskamp RMJ, Ruysschaert JM, Ryan JF, Separovic F, Watts A. J Mol Biol. 2007; 368:982–997. [PubMed: 17382345]

14. Chimon S, Ishii Y. J Am Chem Soc. 2005; 127:13472–13473. [PubMed: 16190691] Chimon S, Shaibat MA, Jones CR, Calero DC, Aizezi B, Ishii Y. Nat Struct Mol Biol. 2007; 14:1157–1164. [PubMed: 18059284]

15. Tickler AK, Barrow CJ, Wade JD. J Pept Sci. 2001; 7:488–494. [PubMed: 11587187] Sohma Y, Kiso Y. Chembiochem. 2006; 7:1549–1557. [PubMed: 16915597] Zarandi M, Soos K, Fulop L, Bozso Z, Datki Z, Toth GK, Penke B. J Pept Sci. 2007; 13:94–99. [PubMed: 17103463]

16. Schnolzer M, Alewood P, Jones A, Alewood D, Kent SBH. Int J Pept Protein Res. 1992; 40:180–193. [PubMed: 1478777] Canne LE, Botti P, Simon RJ, Chen Y, Dennis EA, Kent SBH. J Am Chem Soc. 1999; 121:8720–8727.Dawson PE, Kent SBH. Annu Rev Biochem. 2000; 69:923–960. [PubMed: 10966479]

17. Baldus M. Curr Opin Struct Biol. 2006; 16:618–623. [PubMed: 16942870] McDermott AE. Annu Rev Biophys. 2009; 38:385–403. [PubMed: 19245337] Jaroniec CP, MacPhee CE, Astrof NS, Dobson CM, Griffin RG. Proc Natl Acad Sci U S A. 2002; 99:16748–16753. [PubMed: 12481032] Castellani F, van Rossum B, Diehl A, Schubert M, Rehbein K, Oschkinat H. Nature. 2002; 420:98–102. [PubMed: 12422222] Lange A, Giller K, Hornig S, Martin-Eauclaire MF, Pongs O, Becker S, Baldus M. Nature. 2006; 440:959–962. [PubMed: 16612389] Pintacuda G, Giraud N, Picrattelli R, Bockmann A, Bertini I, Emsley L. Angew Chem Int Edit. 2007; 46:1079–1082.Curtis-Fisk J, Spencer RM, Weliky DP. J Am Chem Soc. 2008; 130:12568. [PubMed: 18759389] Helmus JJ, Surewicz K, Nadaud PS, Surewicz WK, Jaroniec CP. Proc Natl Acad Sci U S A. 2008; 105:6284–6289. [PubMed: 18436646] Wasmer C, Lange A, Van Melckebeke H, Siemer AB, Riek R, Meier BH. Science. 2008; 319:1523–1526. [PubMed: 18339938] Cady SD, Schmidt-Rohr K, Wang J, Soto CS, DeGrado WF, Hong M. Nature. 2010; 463:689-U127. [PubMed: 20130653] Bertini I, Luchinat C, Parigi G, Ravera E, Reif B, Turano P. Proc Natl Acad Sci U S A. 2011; 108:10396–10399. [PubMed: 21670262]

18. Ishii Y. J Chem Phys. 2001; 114:8473–8483.

19. Petkova AT, Ishii Y, Balbach JJ, Antzutkin ON, Leapman RD, Delaglio F, Tycko R. Proc Natl Acad Sci U S A. 2002; 99:16742–16747. [PubMed: 12481027]

20. Riek R, Guntert P, Dobeli H, Wipf B, Wuthrich K. European Journal of Biochemistry. 2001; 268:5930–5936. [PubMed: 11722581]

21. Tycko RQ. Rev Biophys. 2006; 39:1–55.

22. Spera S, Bax A. J Am Chem Soc. 1991; 113:5490–5492.

23. Cornilescu G, Delaglio F, Bax A. J Biomol NMR. 1999; 13:289–302. [PubMed: 10212987]

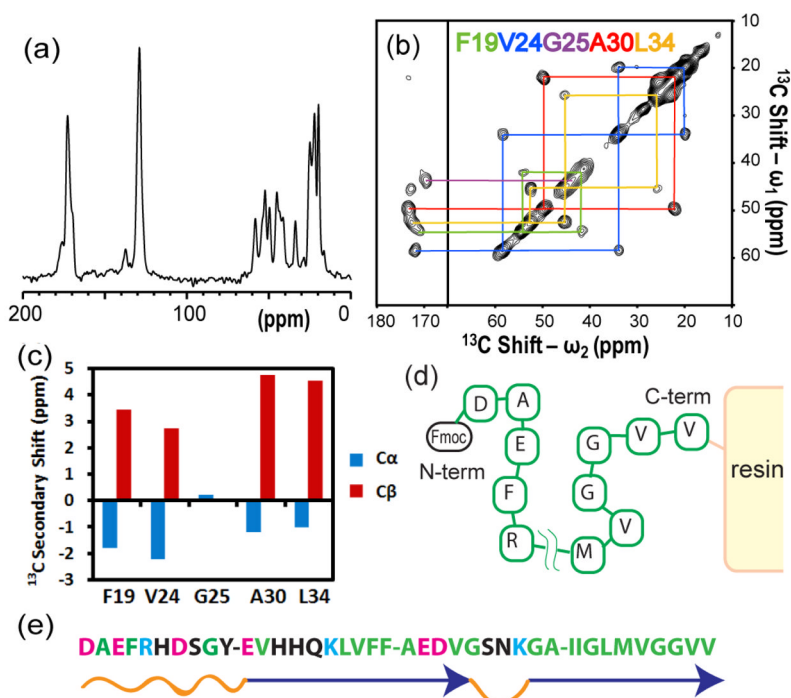24. Fields CG, Fields GB, Noble RL, Cross TA. Int J Pept Protein Res. 1989; 33:298–303. [PubMed: 2473960]

**Figure 1.**
(a) 1D $^{13}$C CPMAS spectrum and (b) 2D $^{13}$C/$^{13}$C correlation SSNMR spectrum of resin-bound Aβ (1-40) solvated with dichloromethane (DCM) with color-coded signal assignments (see the inset). The spinning speed was 20 kHz. The peptide was synthesized with uniformly $^{13}$C- and $^{15}$N-labeled amino acids at Phe-19, Val-24, Gly-25, Ala-30, and Leu-34. For synthesis of the sample, a standard Fmoc SPPS protocol was employed using N-Methyl-2-pyrrolidone (NMP) as a solvent and Fmoc-Val-Wang resin (0.22 meq/g) swollen with DCM. The resin was washed with DCM at the end of the synthesis. The data acquisition for (a) was started ca. 2 h after the synthesis. In (a, b), during the CP period, the $^{13}$C RF field amplitude was linearly swept from 46 kHz to 63 kHz during a contact time of 1.0 ms, while the $^1$H RF amplitude was kept constant at 75 kHz. In (a), the experimental time was 17 min. The spectrum in (b) was obtained with an fpRFDR sequence.[18] During a mixing period, fpRFDR $^{13}$C-$^{13}$C dipolar recoupling sequence with a mixing time of 1.6 ms and $^{13}$C π-pulse widths of 15 μs was used. The experimental time for (b) was 19 h. (c) $^{13}$C secondary chemical shift analysis of Phe-19, Val-24, Gly-25, Ala-30, and Leu-34 for Aβ (1-40) bound to Aβ resin. (d) A schematic representation of an Aβ peptide bound to resin. (e) The amino-acid sequence of Aβ (1-40) peptide and the secondary structure suggested by SSNMR for the amyloid fibril,[19] where blue arrows denote β-sheet regions and orange loops denote unstructured or loop regions.
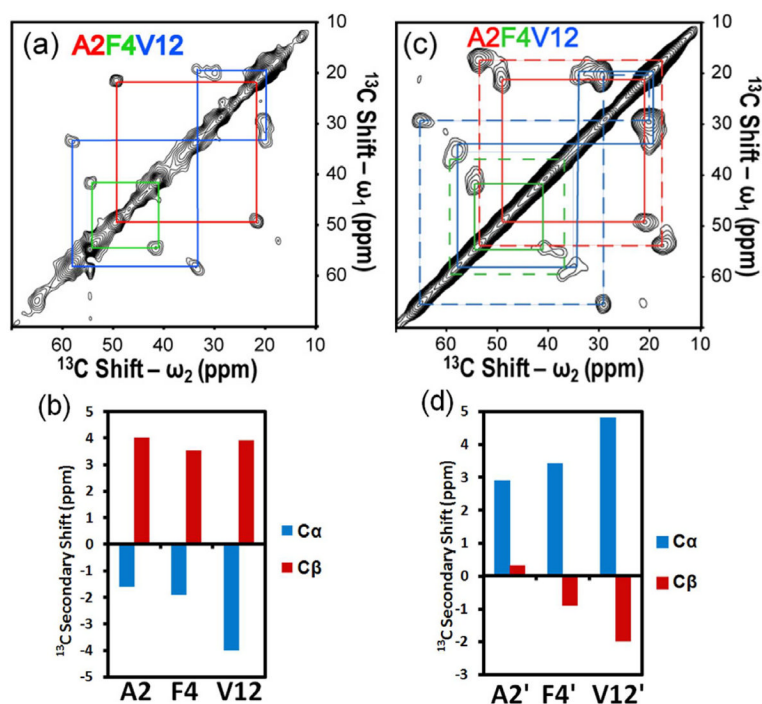
**Figure 2.**
(a) The aliphatic region of a 2D $^{13}$C/$^{13}$C chemical-shift correlation SSNMR spectrum of a resin-bound Aβ (1-40) solvated with dichloromethane (DCM) with color-coded signal assignments (red: Ala-2; green: Phe-4; blue: Val-12). The peptide was labeled with uniformly $^{13}$C- and $^{15}$N-labeled amino acids at Ala-2, Phe-4, and Val-12. The sample preparation and SSNMR method are the same as those in Fig. 1b except for the labeled positions. The experimental time was 31 h. (b) A $^{13}$C secondary chemical shift analysis of Ala-2, Phe-4, and Val-12 for Aβ (1-40) bound to Aβ resin. (c) The aliphatic region of a 2D $^{13}$C/$^{13}$C correlation SSNMR spectrum for the same resin-bound Aβ (1-40) sample after the removal of DCM with color-coded assignments. Dashed lines show the new resonances that appeared after removal of DCM. The experimental time was 31 h. (d) The $^{13}$C secondary chemical shift analysis of the new resonances of Ala-2, Phe-4, and Val-12 for the dried resin-bound Aβ (1-40) sample used in (c).